AJNR

This information is current as of August 12, 2025.

High-Resolution MR Imaging of Sequestered Lumbar Intervertebral Disks

Thomas J. Masaryk, Jeffrey S. Ross, Michael T. Modic, Francis Boumphrey, Henry Bohlman and Geoffrey Wilber

High-Resolution MR Imaging of Sequestered Lumbar Intervertebral Disks

Thomas J. Masaryk[1]
Jeffrey S. Ross[1]
Michael T. Modic[1]
Francis Boumphrey[2]
Henry Bohlman[3]
Geoffrey Wilber[3]

We retrospectively reviewed the MR examinations of 20 patients with surgically documented sequestered lumbar disks (free fragments). Sixteen of 20 cases demonstrated extradural masses that were distinct from the interspace of origin and had intermediate signal on T1-weighted images but increased signal on T2-weighted images. In 12 cases there was migration of the sequestered fragment. Sequestered disks that migrated away from the interspace had an irregular, oblong appearance, while those near the interspace were round in configuration. Additionally, the interspace of origin consistently demonstrated loss of signal on T2-weighted images when compared with intact lumbar disks. Sagittal 12-weighted images best depicted the absence of a high-signal pedicle contiguous with the interspace of origin in sequestered disks. These findings were applied to a prospective group of 20 patients undergoing lumbar diskectomy. There was an 89% sensitivity, 82% specificity, and 85% accuracy for MR in distinguishing sequestered disks from other forms of lumbar disk herniation.

We conclude that high-resolution MR imaging is sensitive in detecting disk disease and specific in characterizing various subtypes of extradural defects. MR uses morphology as well as changes in signal intensity to make these distinctions.

One of the earliest stated advantages of MR imaging of the lumbar spine is its ability to screen for degenerative disk disease, the underlying process behind disk herniation. This was often recognized on early body-coil images (using a 15-mm image thickness) as a loss of signal intensity from within the disk on T2-weighted images [1, 2]. That observation led to the statement that "while not all degenerated discs herniate, all herniated discs eventually degenerate"; the implication being that herniated disks generally demonstrate low signal intensity on T2-weighted images [1]. With the development of high-resolution surface-coil MR imaging, many radiologists have come to recognize that certain forms of disk herniation are often associated with low- or intermediate-signal-intensity extradural defects on T1-weighted images, which are high signal on spin-density and T2-weighted images. In particular, sequestered disks (free fragments) have been recognized by several investigators as high-signal, soft-tissue masses distinctly separate from the parent interspace on T2-weighted images [3–5]. Diagnosis of sequestered disks is clinically important and may affect patient management and mode of therapy [6–11].

The objective of this study was to: (1) define the surface-coil MR characteristics of sequestered disks, (2) determine the ability of surface-coil MR to reliably distinguish sequestered disks (free fragments) from other forms of disk rupture, and (3) compare the ability of surface-coil MR with that of CT myelography to make this distinction. Note that the purpose was not to compare surface-coil MR with CT myelography in the diagnosis of degenerative disk disease per se, as this has been specifically addressed in a previous publication [4].

Materials and Methods

This study is divided into two parts. In the first, in an effort to evaluate the surface-coil MR findings of sequestered disks, we retrospectively reviewed the surface-coil MR studies in 20

cases of surgically proved sequestered disks accumulated over a 2-year period. Subsequently, we applied these findings prospectively to patients undergoing lumbar diskectomy who preoperatively had surface-coil MR and CT myelography.

Retrospective

The patient population in our retrospective review of 20 cases of surgically proved sequestered disks consisted of 13 men and seven women ranging in age from 26 to 66 years. All patients demonstrated extradural defects with a decrease in the adjacent interspace height.

Thirteen of the MR retrospective examinations were performed on a 0.6-T superconductive unit (Teslacon, Technicare) using a prototype surface coil. The surface coil was circular, 12 cm in diameter, and composed of 5/8 in. copper tubing. It served as a receiver only; a 50-cm body coil served as the RF transmitter.

Seven of the retrospective surface-coil MR examinations were performed on a 1.5-T superconductive unit (Siemens Magnetom) using a prototype 12-cm, circular, wrapped-copper-foil surface coil. This coil likewise served as the receiver only. A 50-cm body coil served as the RF transmitter.

The surface-coil MR studies consisted of four separate spin-echo sequences. The first was a coronal scout, TR = 500 msec, TE = 30 msec, 1-cm-thick section, 128 × 128 matrix, one excitation, and an imaging time of 1.1 min. This sequence allowed accurate orientation and positioning of the surface coil. The second sequence was a sagittal image, TR = 500 msec, TE = 15–30 msec two excitations yielding seven to 12 4-mm-thick sections, and an imaging time of 4.4 min. The third sequence was a sagittal image, TR = 2000 msec, TE = 60–90 msec, one to two excitations yielding 12 4-mm-thick sections, and an imaging time of 9–18 min. The fourth sequence was a multiecho axial image, TR = 2000 msec, TE = 30–60 msec, one to two excitations yielding 4-mm-thick sections, and an imaging time of 9–18 min. The second through fourth sequences used a 1-mm gap between image sections and a 128 × 256 or 256 × 256 matrix.

Retrospective reviews of the surface-coil MR images in cases of sequestered lumbar disks were evaluated for size, morphology (round, elliptical, or polypoid), location of extradural defects, and signal intensity on short TR/TE (T1-weighted) and long TR/TE (T2-weighted) images. Note was made of the suspected interspace of origin, its posterior margin, and presence or absence of migration (superior, inferior). Signal intensity of the extradural defect and adjacent interspace was compared with that of intact lumbar intervertebral disks (i.e., those demonstrating negligible interspace narrowing, no evidence of bulging anulus or herniation, and increased signal intensity on T2-weighted images) on T2-weighted images, usually at the L1–L2 or L2–L3 levels. Using an electronic cursor, we obtained region of interest signal intensity measurements of the extradural defect and adjacent interspace, intact intervertebral disks, and background noise. After correcting for background noise, we obtained ratios of the signal of the extradural defect and intervertebral disk of origin to the signal of the intact intervertebral disks. After the data were collected, a surface-coil MR classification scheme for the various extradural defects of lumbar degenerative disk disease was developed for use in the prospective group.

Prospective

The second part of the study consisted of a prospective comparison of surface-coil MR imaging vs CT myelography to determine the ability of each to distinguish sequestered from nonsequestered disks in patients with known lumbar spine degenerative disk disease. This group consisted of 11 women and nine men (ages 18 to 73). The

goal of the study was to obtain parallel surface-coil MR imaging and CT myelography examinations in 20 surgically confirmed herniated disks.

Patients who presented with signs and symptoms of lumbar radiculopathy were admitted to the study. Patients' diagnostic workups included a lumbar myelogram with water-soluble contrast material followed immediately by CT myelography. All surface-coil MR studies were performed within 1 week of the myelogram and CT scan. The CT myelograms and surface-coil MR studies were interpreted independently, without knowledge of the results of the other study. Using the criteria defined by the retrospective group, we classified extradural defects as either sequestered disks (free fragments) or "other" (e.g., bulging anulus, prolapsed, extruded). Subsequently, imaging results were compared with surgical findings according to the same classification criteria.

For the prospective part of the study all MR examinations were performed on a 1.5 T superconductive unit (Siemens Magnetom) in the same fashion as described for the retrospective study.

Using the findings in the retrospective group, as well as previous MR experience in the diagnosis of lumbar disk disease, we adapted the classification scheme used by the surgical services in their operative reports after Macnab [12–14]. Following are definitions for degenerated and/or herniated disks that were subsequently applied to the prospective group.

(1) Bulging disks (Fig. 1) are the result of disk degeneration with an intact anulus, usually recognized as a generalized extension of the disk margin beyond the margins of the adjacent vertebral endplates, regardless of the signal from the interspace. On T2-weighted images the darker Sharpey's fibers remain intact.

(2) Prolapsed disks (Fig. 2) are the result of herniation of nuclear material through a defect in the anulus producing focal extension of the disk margin. Herniated material is contiguous with the parent nucleus via a recognizable pedicle of higher signal extending beyond the endplates on T2-weighted sagittal images. The displaced nuclear material is confined by a few of the low-signal outer fibers of the anulus that may be seen as a demarcating line of low signal between the defect and epidural fat/thecal sac. Signal intensity of the extradural defect may be increased or decreased on T2-weighted images.

(3) Extruded disks (Fig. 3) are the result of herniation of nuclear material producing an anterior extradural mass that remains attached to the nucleus of origin via a high-signal pedicle on T2-weighted images. The lesion is no longer bounded by the outer anulus and may lie beneath or lateral to the posterior longitudinal ligaments. The extradural defect often possesses higher signal than (and thus can be distinguished from) the adjacent outer anulus. Care must be taken to distinguish chemical shift boundary effects from outer anular fibers when attempting to distinguish between prolapsed and extruded disks [15]. In Figure 3B the frequency-encoded gradient is aligned vertically. Knowing this, it would be difficult with this image alone to distinguish low-signal outer anulus from chemical shift effect at the superior border of the extradural defect. This is less a problem on the T2-weighted image (Fig. 3C). Should confusion persist, the scan may be repeated with the frequency and phase-encoded directions reversed [15].

(4) Sequestered disks (Fig. 4) are the result of herniation of nuclear material through a defect in the anulus that is no longer contiguous with the remaining disk. The isolated fragment is thus "sequestered," and is also called a "free" fragment. These fragments may lie anterior or posterior to the posterior longitudinal ligament, inferior or superior to the interspace, and typically have a signal intensity that is at least 70% greater than that of remaining intact lumbar disks on T2-weighted images.

CT myelography was performed after plain film myelography using 12–17 ml of contrast material (180 mg iohexol per ml) instilled
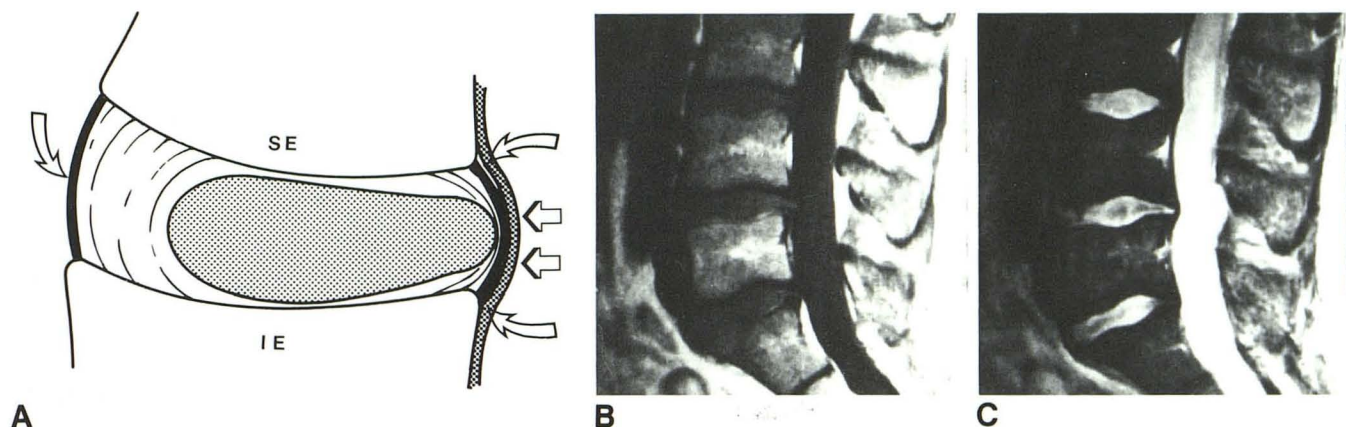
Fig. 1.—*A*, Diagram shows bulging anulus fibrosus as a generalized extension of disk margin beyond boundary of adjacent vertebral body endplates. SE = superior endplate, IE = inferior endplate, *curved arrows* = outer anular fibers, *straight arrows* = posterior longitudinal ligament. Circumferential lines and shaded area represent high-signal nucleus/inner anular complex, which, on T2-weighted images, cannot be separated.

B, T1-weighted midline sagittal image of lower lumbar spine shows anterior extradural defect at L4–L5 level.

C, T2-weighted midline sagittal image of lower lumbar spine again demonstrates mild anterior extradural defect at L4–L5 level. Note that nucleus/inner anular complex is bounded by dark Sharpey's fibers posteriorly. There is no focal extension of high-signal disk material beyond interspace.
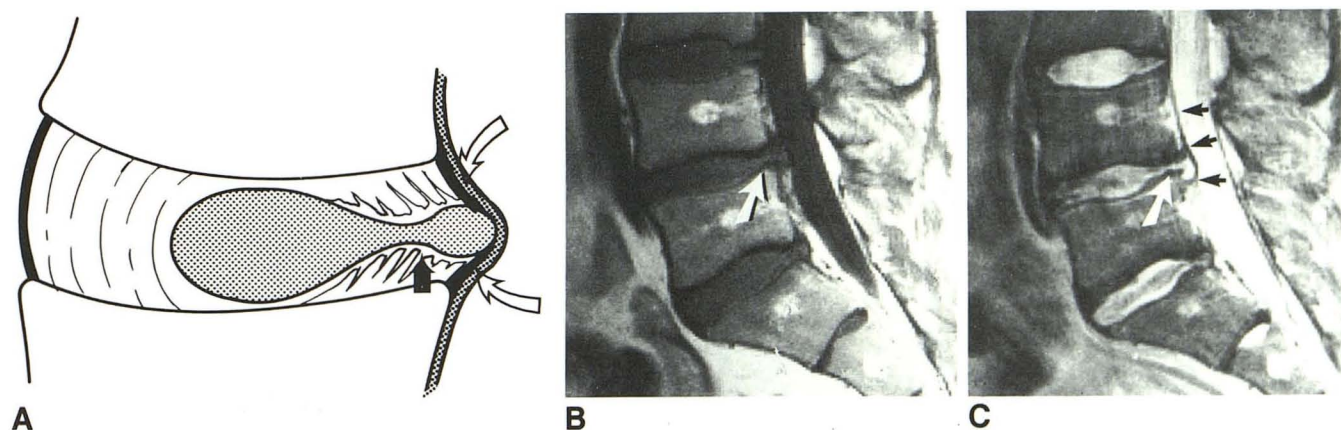

Fig. 2.—*A*, Diagram shows disk prolapse as focal extension of disk margin in which nuclear material has extended through a defect in anulus. Herniated material remains contiguous with parent interspace by a pedicle (*solid arrow*), which may have high signal on T2-weighted images. This prolapsed nuclear material remains confined by outer anular fibers (*open arrows*).

B, T1-weighted midline sagittal image of lower lumbar spine shows focal anterior extradural defect at L4–L5 level. Defect appears to be contiguous with adjacent interspace (*arrow*).

C, T2-weighted sagittal image of lower lumbar spine shows high-signal material from L4–L5 interspace producing an anterior extradural defect, which remains contiguous with interspace via high-signal-intensity pedicle (*white arrow*). However, prolapsed material continues to be bounded by lower-signal-intensity outer anular fibers (*black arrows*).

intrathecally. CT myelography was performed on a Siemens DRH unit using 120 kV and 400–800 mAs. Lateral scout images were obtained in all patients for localization of the axial sections. At least two, and usually three, contiguous 4-mm sections were obtained through the disk region and continued through the adjacent vertebral bodies. Number and locations of scans were determined from the histories and symptoms of the patients, as well as from the findings on the plain film myelographic study.

After the CT myelographic scans were evaluated, abnormal disks were classified as anular bulge, herniated (i.e., prolapsed or extruded), or free fragment according to criteria established in the CT literature [6, 12, 16–18]. (It should be noted here that while the terms "extruded," "extruded fragment," and "free fragment" are occasionally used interchangeably in the radiology literature [6, 16, 17] we reserve the term *extruded* to refer to nuclear material that is extended beyond the outer anulus but that remains contiguous with the parent nucleus. We confine the term *free fragment* or *sequestered fragment* to disk material external to the anulus fibrosus that is no longer contiguous with the parent nucleus.)

Results

Retrospective

In the retrospective group the interspace of origin demonstrated loss of signal on T2-weighted images but appeared
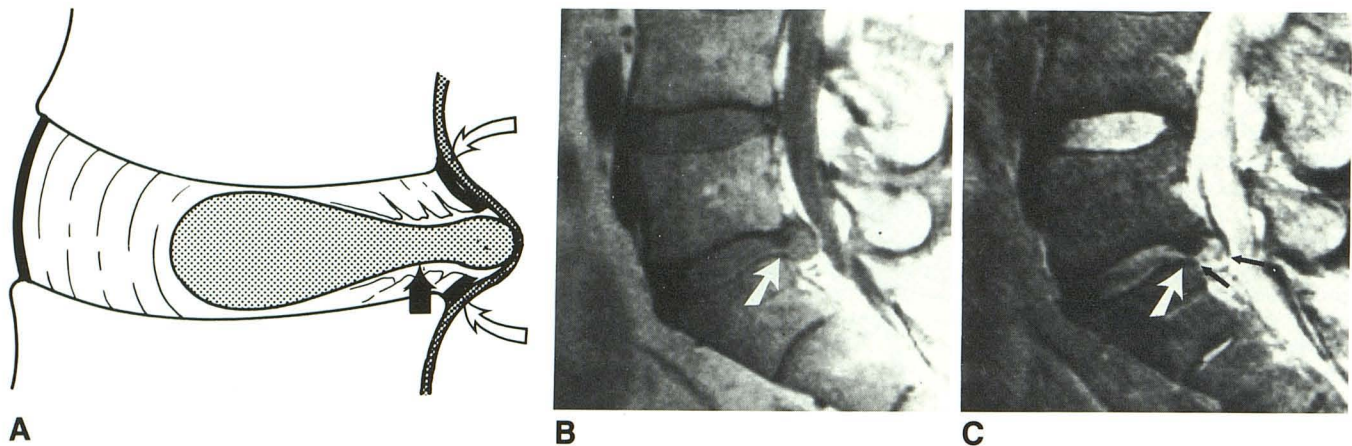
A

B

C

Fig. 3.—*A*, Extruded disk is defined as herniation of nuclear material resulting in anterior extradural mass, which remains attached to nucleus of origin via high-signal pedicle on T2-weighted images (*straight arrow*). Lesion is no longer bounded by outer anular fibers (*curved arrows*) and may lie anterior or lateral to posterior longitudinal ligaments. Extradural defects often possess higher signal than (and thus can be distinguished from) adjacent outer anulus.

B and *C*, T1-weighted (*B*) and T2-weighted (*C*) midline sagittal images of lower lumbar spine. Note large anterior extradural defect at L5–S1 level, which remains contiguous with interspace of origin (*large arrow* in *B* and *C*). Extradural defect is of higher signal than adjacent L5/S1 interspace on T2-weighted study and inferiorly has ruptured through outer anular fibers (*small arrows* in *C*).
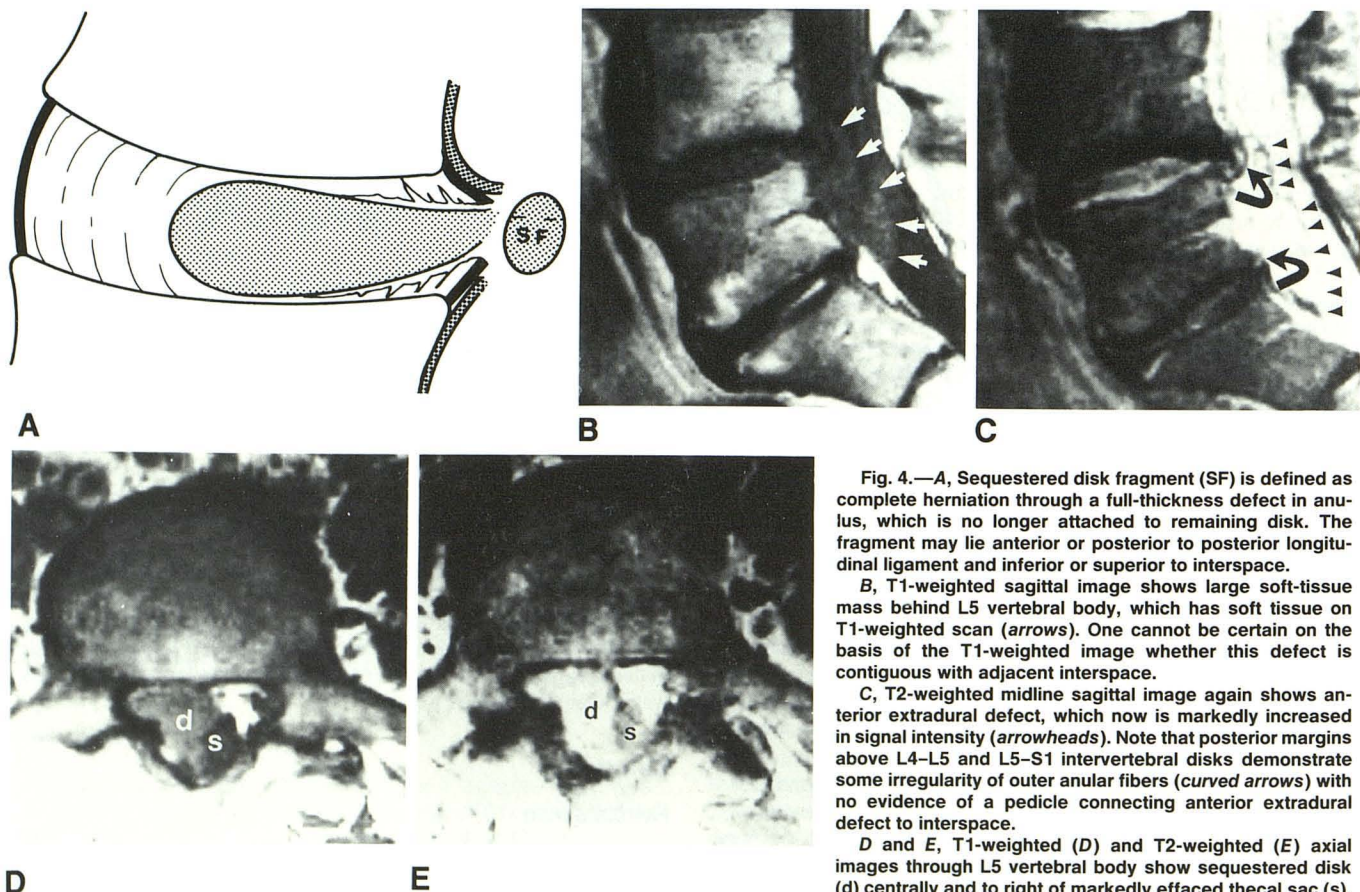

A

B

C

D

E

Fig. 4.—*A*, Sequestered disk fragment (SF) is defined as complete herniation through a full-thickness defect in anulus, which is no longer attached to remaining disk. The fragment may lie anterior or posterior to posterior longitudinal ligament and inferior or superior to interspace.

B, T1-weighted sagittal image shows large soft-tissue mass behind L5 vertebral body, which has soft tissue on T1-weighted scan (*arrows*). One cannot be certain on the basis of the T1-weighted image whether this defect is contiguous with adjacent interspace.

C, T2-weighted midline sagittal image again shows anterior extradural defect, which now is markedly increased in signal intensity (*arrowheads*). Note that posterior margins above L4–L5 and L5–S1 intervertebral disks demonstrate some irregularity of outer anular fibers (*curved arrows*) with no evidence of a pedicle connecting anterior extradural defect to interspace.

D and *E*, T1-weighted (*D*) and T2-weighted (*E*) axial images through L5 vertebral body show sequestered disk (d) centrally and to right of markedly effaced thecal sac (s). Note extremely high signal of extradural defect on this T2-weighted study.

Fig. 5.—*A*, T1-weighted sagittal image shows large anterior extradural defect at L5/S1 level, which has soft-tissue signal (*arrows*). It is impossible to distinguish anular fibers from herniated nuclear material on the basis of this study.

B, T2-weighted sagittal image of lower lumbar spine again shows anterior extradural defect at L5/S1 level. Frayed posterior anular fibers can now be seen (*arrows*). This is associated with some high-signal material contiguous with interspace of origin anteriorly. However, there is a large high-signal fragment (*arrowheads*) posterior and inferior to anular defect, which is clearly not connected to its native interspace.

A   B
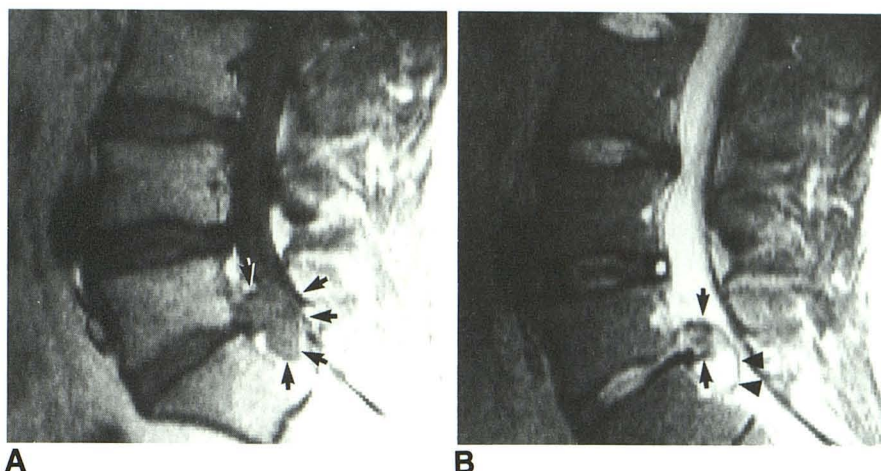
isointense when compared with intact disks on T1-weighted images. Region of interest cursor measurements on T2-weighted images in 12 of these patients demonstrated a mean ratio of signal of interspace of origin to signal of intact lumbar disks of 0.34 ± 0.10 (range, 0.14–0.52). The posterior margin of the interspace of origin was irregular in all cases (Fig. 5). While axial images adequately demonstrated focal defects in the posterior disk margin, sagittal images were better able to establish continuity between the defect and the parent interspace in instances where the fragments had extended above or below the interspace. Likewise, because of differences in signal between the interspace and the fragment on T2-weighted images, the T2-weighted sagittal study was preferable to the T1-weighted sagittal study for distinguishing between sequestered fragments and prolapsed or extruded disks. In particular, these scans were useful in establishing fragments as isolated, high-signal, extradural defects that were frequently separated from the interspace by the frayed, low-signal Sharpey's fibers (Figs. 4 and 5). Sixteen (80%) of 20 cases demonstrated extradural masses that were distinct from the interspace of origin and that had soft-tissue signal on T1-weighted images but increased signal on scans with more T2 weighting. The remaining four cases (20%) likewise demonstrated extradural defects, but they possessed low signal intensity similar to that of the degenerated disks of origin on T2-weighted scans. Region of interest cursor measurements were available in 12 patients and indicated that the mean ratio of fragment signal to signal of intact lumbar disks was 1.17 ± 0.48 (range, 0.35–1.82). Twelve cases demonstrated migration of the sequestered fragment (seven inferior, five superior). Sequestered disks that migrated away from the interspace had an irregular oblong appearance, while those near the interspace were round in configuration.

Prospective

Table 1 presents the comparative findings for surface-coil MR imaging and CT myelography in their ability to distinguish between sequestered lumbar disks and other types of degenerative disk disease in 20 surgical cases examined prospectively. CT myelography produced one false negative and eight

TABLE 1: Comparison of Surface-Coil MR Imaging and CT Myelography in Identifying Sequestered Disks

	Surface-Coil MR Imaging			CT Myelography		
	L4–L5	L5–S1	Total	L4–L5	L5–S1	Total
True positive	4	4	8	4	4	8
False negative		1	1		1	1
True negative	5	4	9	2	3	5
False positive		2	2	3	3	6
Total explorations	9	11	20	9	11	20

true positive diagnoses of sequestered lumbar disks in this group. There were six false positive and five true negative diagnoses in 11 additional cases of other forms of lumbar disk disease. Thus, there was 89% sensitivity, 45% specificity, and 65% accuracy for CT myelography in differentiating between sequestered lumbar disk and other forms of intervertebral disk herniation. Surface-coil MR imaging in the same 20 patients produced one false negative and eight true positive diagnoses of sequestered lumbar disks. There were two false positive and nine true negative diagnoses for other types of lumbar herniation. Overall, there was 89% sensitivity, 82% specificity, and 85% accuracy for surface-coil MR in differentiating between sequestered disks and other forms of lumbar disk herniation.

Discussion

Characterizing and differentiating between the various subgroups of lumbar disk disease has certain diagnostic and therapeutic ramifications. While we recognize that the terminology associated with disk rupture may vary, the terms used in this paper are those used by the radiology and surgical services at our institution and are based on the criteria established by Macnab and others [12–14]. Because of their ability to delineate nucleus/inner anular complex, outer anular fibers, and margins of the adjacent endplates, sagittal T2-weighted images are particularly suited to the application of this scheme [15].

The ability to distinguish between a bulging anulus and a herniated disk is important, inasmuch as a bulging disk is considered to be associated less with sciatica than is a herniated disk [14]. Prolapsed disks are distinguished from extruded disks by the presence of an intact outer anulus [13]. In practice, the true difference is probably a matter of degree of the same lesion. However, recognition of sequestered (free fragment) disks is clinically pertinent as they: (1) may produce misleading localizing signs and symptoms, (2) are a contraindication to the use of chymopapain and percutaneous diskectomy techniques, (3) are a known cause of postoperative back pain, and (4) may require a more extensive surgical approach for complete removal [6–10].

CT compares favorably with myelography in overall diagnostic accuracy, can distinguish bulging anuli from herniated disks, and has the additional advantage of visualizing lateral disk fragments [12, 17, 19–21]. While CT without intrathecal contrast material has been reported as a valuable tool in the detection of free fragments, CT myelography has the added advantage of detecting those large sequestrations that might otherwise be mistaken for the thecal sac [20, 22]. Thus CT myelography has been considered an ideal imaging examination for the evaluation of suspected free fragments, although there are no prospective studies confirming this.

While early body-coil MR imaging did not have the spatial resolution to specifically characterize lumbar disk disease, it did demonstrate signal intensity changes within the interspace on long TR/long TE images, which was thought to be a sensitive indicator of degenerative disk disease [1, 2, 23]. The advent of higher-resolution lumbar MR scanning has resulted in improved sensitivity and specificity for the diagnosis of lumbar disk disease [4]. Likewise, with surface-coil MR imaging one can appreciate signal intensity patterns in sequestered disks that have heretofore been referred to only anecdotally in the literature [3–5]. A frequent finding with free fragments is the presence of high-signal-intensity extradural defects on T2-weighted studies that are distinct and separate from the interspace of origin. This separation is best appreciated on T2-weighted sagittal images, where the contrast between extradural defect and lower-signal outer anulus is greatest. The spatial relationship of the extradural defect to the interspace is best appreciated in the sagittal plane. When the fragments are adjacent to the interspace they have a somewhat rounded configuration, but when superior or inferior to the interspace they frequently appear oval or oblong in configuration. We note that prolapsed or extruded disks may occasionally demonstrate high-signal extradural defects on T2-weighted images, but are distinguished from free fragments by their continuity with the residual nucleus/inner anular complex.

While the purpose of this study was to document the MR findings of sequestered disks and determine the diagnostic reliability of MR imaging, one can speculate as to the possible reasons for the unique appearance of these disks. Pech and Haughton [15] have suggested that gross degeneration of intervertebral disks may be present despite their high signal on long TR/TE images. The consequence of this may be that significant biochemical and/or biomechanical derangement (potentiating herniation) is possible and may lead to the herniation of high-signal material from the interspace on T2-weighted images. Chemical analysis of prolapsed intervertebral disks demonstrates a derangement of the nuclear mucoproteins after herniation, with an eventual reduction of water-binding capacity of the nuclear material [24]. However, in general, sequestered disks appear as large extradural defects (a finding consistent with previous CT descriptions) [6]. It would be reasonable to assume that such large fragments would be symptomatic early in their clinical course, causing the patient to seek medical attention (and to have a diagnostic workup) soon after the onset of symptoms. This is to say, sequestered disks that present early will have a higher water content (i.e., higher spin density and longer T2) than those that present later.

An alternative explanation for the same findings takes into consideration that all the sequestered disks in this series were associated with interspaces that have a lower signal intensity than intact disks on T2-weighted images and assumes that this is a reliable indicator of disk degeneration. It is known that with rupture and loss of confined fluid mechanics within a disk there is initially a reparative process that leads to a transient gain in water content (i.e., spin density) within the disk [24]. Again, assuming an acute clinical presentation, this may be one factor relating to the variable signal seen in different extradural defects. There are also vascular correlations between disk changes and the amount and location of vessels surrounding penetrating areas of disk disease. Hypervascularization likewise appears only during certain phases of disk lesions. The explanations for these observations are as yet not clear but they have been previously interpreted as autoimmune responses to cartilage fractions undergoing degeneration [25, 26]. How these changes affect spin density and T1 and T2 relaxation is open to question.

The differential diagnosis for the surface-coil MR findings of sequestered lumbar disks include epidural abscess, extradural neoplasm (such as neurofibroma), and postoperative epidural fibrosis or fluid collection. Epidural abscesses are frequently associated with disk space infection and can be distinguished from free fragments by the characteristic signal changes seen at the infected interspace and adjacent endplates (Fig. 6) [27]. Extradural tumor may be more difficult to exclude, although multiplicity of lesions and/or the presence of bone marrow changes in instances of metastatic disease would also help to narrow the differential diagnosis. While postoperative scarring in the lumbar spine is typically identified as a loss of signal intensity from the epidural fat, we have seen numerous cases of surgically documented scar that has a high signal intensity on T2-weighted images and that would be difficult to distinguish from a disk fragment (Fig. 7) [28]. The presence (in sequestered disks) or absence (in scar) of mass effect on the thecal sac may help to distinguish the two. Small postoperative fluid collections may mimic high-signal extradural defects on T2-weighted images but usually resolve after 4 to 6 weeks [29]. Parenthetically, most postsurgical collections are posterior to the thecal sac, while all free fragments in this series were ventral to the dura.

Of some concern in this study is the surprisingly large percentage of sequestered disk fragments in the prospective group. A possible explanation may lie in a flawed study design.

Fig. 6.—Serial T1-weighted (A) and T2-weighted (B) images of L4–L5 disk space infection with an epidural abscess (arrow). Note that abscess has similar morphologic and signal characteristics to free fragment seen in Fig. 4. However, the endplate changes (long T1, long T2) helped to distinguish this from a sequestered fragment.
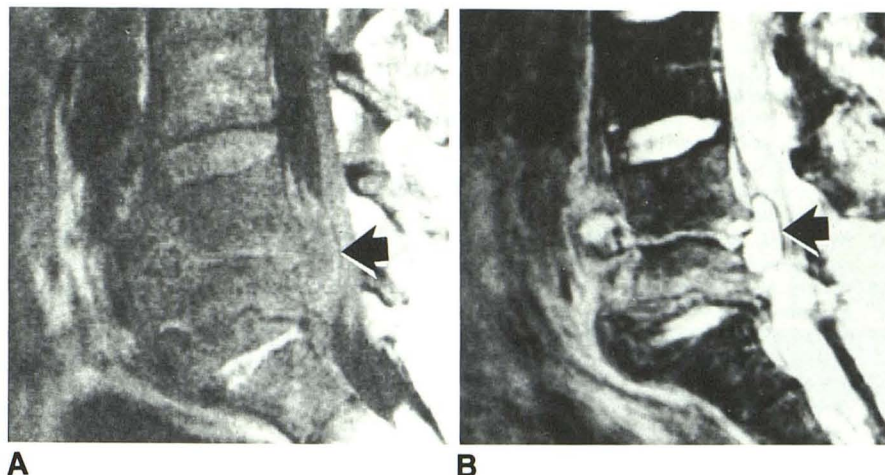
A   B

Fig. 7.—T1-weighted (A) and T2-weighted (B) axial images of L5/S1 disk. Note soft-tissue mass anterior and to right of thecal sac (arrow), which has soft-tissue signal on T1-weighted examination and high signal on T2-weighted study. Note that patient has had a laminectomy. This case represents a surgically documented example of postoperative epidural fibrosis/scar after diskectomy with high signal on T2-weighted study simulating a free fragment.

A   B
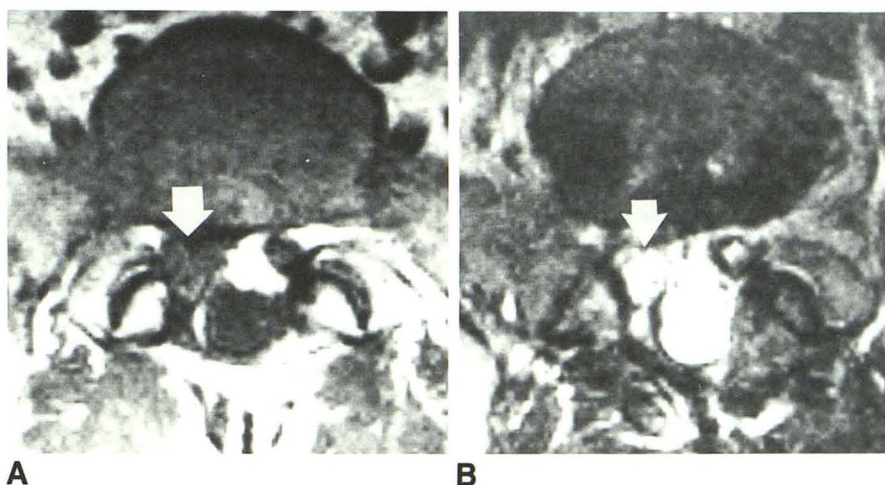
In particular, while the radiologic studies were interpreted independently and prospectively before surgery, the actual referral for the MR examinations was left to the discretion of the surgical services. Inasmuch as they were aware of the findings in the retrospective analysis, there may have been a tendency to preselect for the prospective group those patients who were clinically suspected of having free fragments.

Despite this, a review of the results of this limited study indicate that surface-coil MR imaging is probably equally sensitive to CT myelography for the detection of disk disease, and it is at least as specific for the characterization of various subtypes of extradural defects. MR not only uses morphology but also signal intensity (primarily on T2-weighted sagittal images) to make these distinctions.

REFERENCES

1. Modic MT, Pavlicek W, Weinstein MA, et al. Magnetic resonance imaging of intervertebral disc disease: clinical and pulse sequence considerations. Radiology 1984;152:103–111

2. Chafetz NI, Genant HK, Moon KL, Helms CA, Morris JM. Recognition of lumbar disk herniation with NMR. AJR 1983;141:1153–1156, AJNR 1984;5:23–26

3. Edelman R, Shoukimas GM, Stark DD, et al. High-resolution surface-coil imaging of lumbar disk disease. AJNR 1985;6:479–485

4. Modic MT, Masaryk T, Boumphrey F, Goormastic M, Bell G. Lumbar herniated disk disease and canal stenosis: prospective evaluation by surface coil MR, CT, and myelography. AJNR 1986;7:709–711

5. Masaryk TJ, Boumphrey F, Modic MT, Tamborello C, Ross JS, Brown MD. Effects of chemonucleolysis demonstrated by MR imaging. J Comput Assist Tomogr 1986;10(6):917–923

6. Fries JW, Abodeely DA, Vijungco JG, Yeager VL, Gaffey WR. Computed tomography of herniated and extruded nucleus pulposus. J Comput Assist Tomogr 1982;6(5):874–887

7. Finneson B. Low back pain, 2nd ed. Philadelphia: Lippincott, 1980

8. Smith L. Failures with chemonucleolysis. Orthop Clin North Am 1975;6:255–258

9. Gentry LR, Strother CM, Turski PA, Javid MJ, Sackett JF. Chymopapain chemonucleolysis: correlation of diagnostic radiographic factors and clinical outcome. AJNR 1985;6:311–320

10. Macnab I. Negative disc exploration—an analysis of the course of nerve-root involvement in sixty-eight patients. J Bone Joint Surg [Am] 1971;53:891–903

11. Onik G, Maroon J, Helms C, et al. Automated percutaneous diskectomy: initial patient experiences. Work in progress. Radiology 1987;162:129–132

12. Teplick JG, Haskin ME. CT and lumbar disc herniation. Radiol Clin North

Am **1983**;21(2):259–288

13. Macnab I. *Backache*. Baltimore: Williams & Wilkins **1977**

14. Bosacco SJ, Berman AT. Surgical management of lumbar disc disease. *Radiol Clinic North Am* **1983**;21(2):377–393

15. Pech P, Haughton VM. Lumbar intervertebral disk: correlative MR and anatomic study. *Radiology* **1985**;156:699–701

16. Dillon WP, Kaseff LG, Knackstedt VE, Osborn AG. Computed tomography and differential diagnosis of the extruded lumbar disc. *J Comput Assist Tomogr* **1983**;7(6):969–975

17. Williams AL, Haughton VM, Daniels DL, Grogan JP. Differential CT diagnosis of extruded nucleus pulposis. *Radiology* **1983**;148:141–148

18. Williams AL, Haughton VM, Meyer GA, Ho KC. Computed tomographic appearance of the bulging anulus. *Radiology* **1982**;142:403–408

19. Haughton VM, Elderik OP, Maynaes B, Amundsen P. A prospective comparison of computed tomography and myelography in the diagnosis of herniated lumbar disks. *Radiology* **1982**;142:103–110

20. Firooznia H, Benjamin V, Kircheff II, Ralii M, Golimbu C. CT of lumbar spine disk herniation: correlation with surgical findings. *AJNR* **1984**;5:91–96

21. Williams AL, Haughton VM, Daniels DL, Thornton RS. CT recognition of lateral lumbar disc herniation. *AJNR* **1982**;3:211–213

22. Dublin AB, McGahan JP, Reid MH. The value of computed tomographic

metrizamide myelography in the neuroradiological evaluation of the spine. *Radiology* **1983**;146:79–86

23. Maravilla KR, Lesh P, Weinreb JC, Selby DK, Mooney V. Magnetic resonance imaging of the lumbar spine with CT correlation. *AJNR* **1985**;6:237–245

24. Lipson SJ, Muir H. Protoglycans in experimental intervertebral disc degeneration. *Spine* **1981**;6:194–210

25. Lowther PA, Baxter E. Isolation of a chondroitin sulfate, protein complex from bovine intervertebral disks. *Nature* **1966**;211:595–597

26. Brammark P, Ekholm R, Lundskog J, Hirsch C. Tissue response to chymopapain in different concentrations. Animal investigations on microvascular effects. *Clin Orthop* **1969**;67:52–67

27. Modic MT, Feiglin DH, Piraino DW, et al. Vertebral osteomyelitis: assessment using MR. *Radiology* **1985**;157:157–166

28. Bundschuh CV, Modic MT, Alfidi RJ, Han JS, Bohlman H, Kaufman B. Residual recurrent disc vs postoperative scar in the lumbar spine: assessment in MR. Presented at the annual meeting of the American Roentgen Ray Society, Washington, DC, April **1986**

29. Ross JS, Modic MT, Masaryk TJ, Bohlman H. MR imaging of the postoperative spine. Presented at the annual meeting of the Radiological Society of North America, Chicago, November **1986**